



AFRL-RX-WP-TP-2011-4220

**A NEW CLASS OF SOLID-SOLID PHASE
TRANSFORMATIONS INVOLVING A COMPOSITION-
DEPENDENT DISPLACIVE COMPONENT (PREPRINT)**

S. Nag, A. Devaraj, N. Gupta, S.G. Srinivasan, and R. Banerjee

University of North Texas

R. Srinivasan, R.E.A. Williams, and H.L. Fraser

The Ohio State University

G.B. Viswanathan and J.S. Tiley

Metals Branch

Metals, Ceramics, and NDE Division

S. Banerjee

Department of Atomic Energy and Atomic Energy Commission

JULY 2011

Approved for public release; distribution unlimited.

See additional restrictions described on inside pages

STINFO COPY

**AIR FORCE RESEARCH LABORATORY
MATERIALS AND MANUFACTURING DIRECTORATE
WRIGHT-PATTERSON AIR FORCE BASE, OH 45433-7750
AIR FORCE MATERIEL COMMAND
UNITED STATES AIR FORCE**

REPORT DOCUMENTATION PAGE					Form Approved OMB No. 0704-0188	
The public reporting burden for this collection of information is estimated to average 1 hour per response, including the time for reviewing instructions, searching existing data sources, gathering and maintaining the data needed, and completing and reviewing the collection of information. Send comments regarding this burden estimate or any other aspect of this collection of information, including suggestions for reducing this burden, to Department of Defense, Washington Headquarters Services, Directorate for Information Operations and Reports (0704-0188), 1215 Jefferson Davis Highway, Suite 1204, Arlington, VA 22202-4302. Respondents should be aware that notwithstanding any other provision of law, no person shall be subject to any penalty for failing to comply with a collection of information if it does not display a currently valid OMB control number. PLEASE DO NOT RETURN YOUR FORM TO THE ABOVE ADDRESS.						
1. REPORT DATE (DD-MM-YY) July 2011		2. REPORT TYPE Journal Article Preprint		3. DATES COVERED (From - To) 01 July 2011 – 01 July 2011		
4. TITLE AND SUBTITLE A NEW CLASS OF SOLID-SOLID PHASE TRANSFORMATIONS INVOLVING A COMPOSITION-DEPENDENT DISPLACIVE COMPONENT (PREPRINT)				5a. CONTRACT NUMBER FA8650-08-C-5226		
				5b. GRANT NUMBER		
				5c. PROGRAM ELEMENT NUMBER 62102F		
6. AUTHOR(S) S. Nag, A. Devaraj, N. Gupta, S.G. Srinivasan, and R. Banerjee (University of North Texas) R. Srinivasan, R.E.A. Williams, and H.L. Fraser (The Ohio State University) G.B. Viswanathan and J.S. Tiley (AFRL/RXLM) S. Banerjee (Department of Atomic Energy and Atomic Energy Commission)				5d. PROJECT NUMBER 4349		
				5e. TASK NUMBER 00		
				5f. WORK UNIT NUMBER LM114100		
7. PERFORMING ORGANIZATION NAME(S) AND ADDRESS(ES) <div style="display: flex; border-bottom: 1px dashed black; padding-bottom: 5px;"> <div style="flex: 1;">University of North Texas Denton, TX 76203</div> <div style="flex: 1;">Metals Branch (AFRL/RXLM) Metals, Ceramics, and NDE Division Air Force Research Laboratory Materials and Manufacturing Directorate Wright-Patterson Air Force Base, OH 45433-7750 Air Force Materiel Command, United States Air Force</div> </div> <div style="border-bottom: 1px dashed black; padding-bottom: 5px;"> <div style="flex: 1;">The Ohio State University Columbus, OH 43210</div> <div style="flex: 1;">Department of Atomic Energy and Atomic Energy Commission Mumbai, India</div> </div>				8. PERFORMING ORGANIZATION REPORT NUMBER		
9. SPONSORING/MONITORING AGENCY NAME(S) AND ADDRESS(ES) Air Force Research Laboratory Materials and Manufacturing Directorate Wright-Patterson Air Force Base, OH 45433-7750 Air Force Materiel Command United States Air Force				10. SPONSORING/MONITORING AGENCY ACRONYM(S) AFRL/RXLM		
				11. SPONSORING/MONITORING AGENCY REPORT NUMBER(S) AFRL-RX-WP-TP-2011-4220		
12. DISTRIBUTION/AVAILABILITY STATEMENT Approved for public release; distribution unlimited.						
13. SUPPLEMENTARY NOTES PAO Case Number: 88ABW 2011-1188; Clearance Date: 09 Mar 2011. Document contains color. Journal article submitted from publication in <i>Physics Review Letters</i> .						
14. ABSTRACT Solid-solid displacive, structural phase transformations typically undergo a discrete structural change from the parent to the product phase. Coupling electron microscopy, three-dimensional atom probe, and first-principles computations, we present the first direct evidence of a novel mechanism for a coupled diffusional-displacive transformation in an important class of titanium-molybdenum alloys wherein the displacive component in the product phase changes continuously, as a function of its composition. These results cannot be explained by conventional theories and have wide implications.						
15. SUBJECT TERMS solid-solid displacive, coupling electron microscopy, coupled diffusional-displacive transformation, titanium-molybdenum						
16. SECURITY CLASSIFICATION OF:			17. LIMITATION OF ABSTRACT: SAR	18. NUMBER OF PAGES 10	19a. NAME OF RESPONSIBLE PERSON (Monitor) Jaimie S. Tiley 19b. TELEPHONE NUMBER (Include Area Code) N/A	
a. REPORT Unclassified	b. ABSTRACT Unclassified	c. THIS PAGE Unclassified				

A New Class of Solid-Solid Phase Transformations Involving a Composition-Dependent Displacive Component

S. Nag¹, A. Devaraj¹, R. Srinivasan², R. E. A. Williams², N. Gupta¹, G. B. Viswanathan³, J. S. Tiley³, S. Banerjee⁴, S. G. Srinivasan¹, H. L. Fraser², and R. Banerjee^{1*}

¹ *Department of Materials Science and Engineering, University of North Texas, Denton, USA*

² *Department of Materials Science and Engineering, The Ohio State University, Columbus, USA*

³ *Materials and Manufacturing Directorate, Air Force Research Laboratory, Dayton, USA, and*

⁴ *Department of Atomic Energy and Atomic Energy Commission, Mumbai, India.*

(Dated: March 2, 2011)

Solid-solid displacive, structural phase transformations typically undergo a discrete structural change from the parent to the product phase. Coupling electron microscopy, three-dimensional atom probe, and first-principles computations, we present the first direct evidence of a novel mechanism for a coupled diffusional-displacive transformation in an important class of titanium-molybdenum alloys wherein the displacive component in the product phase changes continuously, as a function of its composition. These results cannot be explained by conventional theories and have wide implications for numerous other solid-solid transformations.

Solid-solid phase transformations are ubiquitous in nature and fundamental to modern materials science. The so-called first-order transformations involve discrete nucleation and growth of the product phase in the parent phase matrix, while second (or higher) order ones involve a homogeneous continuous transformation from the parent to the product phases. Importantly, classical nucleation theory of first-order transformations assume that the second phase nucleus has the equilibrium composition and crystal structure of the product phase. The first-order transformations are further classified as diffusional, displacive, and coupled diffusional-displacive (mixed-mode) depending on the operative transformation mechanism. Mixed-mode transformations, such as the classical bainite transformation in steels, typically include coupled diffusional and displacive (often shear or shuffle-based) components. The Bainite transformation in the Fe-C system involves decomposition of a face-centered cubic (fcc) parent phase (γ) into a body-centered cubic (bcc) α and orthorhombic cementite (Fe_3C) phases via diffusive partitioning of carbon followed by a displacive change in crystal structure. Importantly, this γ to α and similar first-order transformations, are believed to involve a single discrete step over an activation energy barrier. This letter, for the first time, presents evidence for a new mixed-mode solid-solid transformation wherein both a diffusive compositional change and a displacive structural change occur in a coupled yet continuous fashion, thus displaying features of a second-order transformation while still being a first order transformation. Our proposed mechanism explains the observed partially transformed embryos, lying in between the two end states, associated with local minima in the free energy landscape of the system.

This new transformation mechanism has been observed for the bcc (β) to the hexagonal ω phase transformation, directly relevant to a wide variety of important en-

gineering alloys involving Group IV elements. At ambient pressure, titanium (Ti), zirconium (Zr), hafnium (Hf), and other Group IV elements exhibit two distinct allotriomorphs – stable low temperature hexagonal close-packed (hcp) α and stable higher temperature bcc β phases. Alloys of these elements, containing a critical concentration of β -stabilizing elements, form a metastable, non-close packed hexagonal ω phase upon rapidly cooling from the high temperature single β phase field followed by isothermal annealing [1]. The ω phase has been actively studied for over 50-years due to its complex formation mechanism and also because it influences mechanical and superconducting properties [2–5]. It is now widely accepted that athermal ω precipitates retain the composition of the parent β matrix, and have been postulated to form by a purely displacive collapse of the $\{111\}$ planes of the bcc phase via a shuffle mechanism [6, 7]. In contrast, the isothermal ω precipitates have been postulated to form via a thermally-activated process involving diffusion-based compositional partitioning followed by the collapse of $\{111\}$ bcc planes in the compositionally-depleted regions [6, 7].

In this letter, we present the salient aspects of the newly proposed transformation mechanism using titanium-molybdenum (Ti-Mo) alloys as a model system. Experiments show evidence of concurrent compositional and structural instabilities within the undercooled bcc β phase of a Ti-Mo alloy leading to the formation of embryos with partially transformed ω -like structures. Nanometer-scale molybdenum-depleted pockets, arising from the early stages of phase separation (clustering) within the β matrix, have been qualitatively detected using aberration-corrected high-resolution scanning transmission electron microscopy (HRSTEM) and quantitatively measured by three-dimensional atom probe (3DAP). The concurrent structural instabilities lead to the partial collapse of $\{111\}\beta$ planes within these Mo-depleted pockets, leading to the formation of embryonic

*Email: banerjee@unt.edu

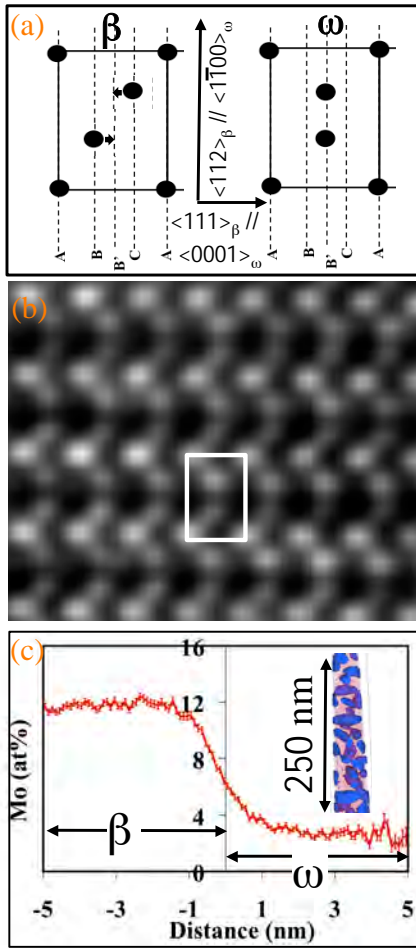


FIG. 1: (a) Schematic arrangement of atoms as seen from $\langle 110 \rangle_\beta$ zone axis, along with the β and fully collapsed ω motifs in a $475^\circ\text{C}/30$ minutes aged Ti-9at%Mo sample. Small arrows show the shifts of atoms along $\langle 111 \rangle_\beta$ directions. (b) HRTEM image recorded along $\langle 011 \rangle_\beta$ zone axis showing the collapse in atomic columns corresponding to well developed ω phase. (c) Proximity histogram using Ti=93 at% isosurface that shows substantial compositional partitioning between the β and ω phases. Inset shows the corresponding 3DAP reconstruction exhibiting the Ti-rich regions.

ω -like structures, which have been directly imaged at atomic resolution using aberration-corrected HRSTEM. Finally, first-principles electronic-structure based computations reveal that these partially transformed ω -like structures correspond to local energy minima in the free energy landscape and are composition-dependent transition states between the parent β and the fully transformed ω structures.

Samples of forged and annealed Ti-9at%Mo (18wt% Mo) alloy from the TIMETALTM company, were solution heat-treated in the single β phase field at 1000°C for 30 minutes in a vacuum furnace ($\sim 1 \times 10^{-6}$ torr) and then rapidly cooled at $\sim 10^\circ\text{C}/\text{sec}$ in Ar gas. Some of these rapidly cooled samples were subsequently annealed at 475°C for 30 minutes. Specimens prepared for transmission electron microscopy via the FEI Nova Nanolab

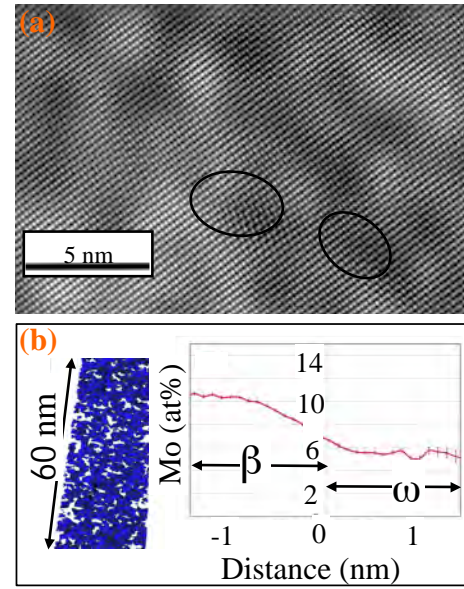


FIG. 2: (a) Filtered HAADF-HRSTEM image of rapidly cooled Ti-9at%Mo sample recorded along $\langle 011 \rangle_\beta$ zone axis showing the atomic columns within the bcc matrix as well as marked regions corresponding to the ω embryos. (b) 3DAP atomic reconstruction of Ti-rich regions as iso-concentration surfaces (Ti = 93 at%). Corresponding proximity histogram shows the compositions of solute-rich and solute-lean regions.

200 dual-beam Focused Ion Beam (FIB) system were analyzed in a FEI Tecnai F20-FEG TEM. The FIB was also used to prepare samples for 3D atom probe (3DAP) studies [8], carried out in a local electrode atom probe (LEAPTM) system from Cameca Instruments Inc. The samples were run in electric-field evaporation mode at a temperature of 70K, with an evaporation rate of 0.2–1.0 % and a voltage pulse fraction at 20% of the steady-state applied voltage. Atomic resolution, Z-contrast, imaging (through High Angle Annular Dark Field (HAADF)-HRSTEM) was performed on a FEI Titan 80-300 microscope, operated at 300 kV, equipped with a CEOS probe aberration corrector.

Well-developed 30–50 nm sized ω precipitates (not shown) have been observed in the Ti-9at%Mo sample that was β solutionized (at 1000°C), quenched, and then isothermally annealed for 30 mins at 475°C . The displacement of atomic columns within the bcc phase, equivalent to the collapse of the $\{111\}_\beta$ planes, leading to the formation of ω phase is illustrated by the schematic β -motif in Fig.1a, and has been discussed in the literature [1, 6, 7]. This fully developed ω structure, is clearly visible in the atomic-resolution TEM image shown in Fig. 1(b) from the 475°C annealed Ti-9at%Mo sample. The same sample has also been analyzed using 3D atom probe and a tomographic reconstruction of the ω precipitates, defined by a 93at% Ti-rich iso-concentration surface, together with Mo atoms in red is shown as an inset in Fig. 1(c)[9]. The compositional partitioning of Mo across the $\beta - \omega$ interface is shown in the same figure as a prox-

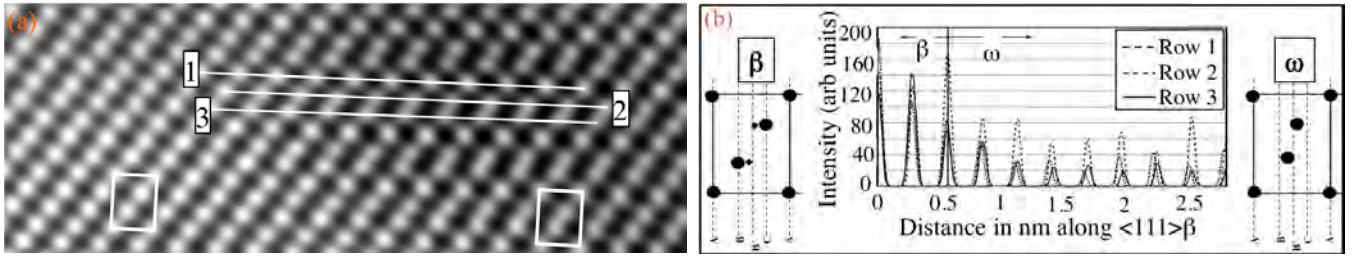


FIG. 3: (a) Enlarged HAADF-HRSTEM image of rapidly cooled Ti-9at%Mo sample showing the un-displaced and partially displaced atomic columns within the β matrix and ω embryo respectively. On (a) three consecutive $\langle 111 \rangle$ β columns have been marked in order to calculate the atomic displacements. (b) The plot in the center shows the column intensities along rows 1, 2 and 3 (as shown in (a)) as a function of distance along the $\langle 111 \rangle$ β directions. On both sides of the plot, cartoons show the arrangement of atoms as seen from $\langle 110 \rangle$ β zone axis, along with the β and partially collapsed ω motifs. Small arrows show the shifts of atoms along $\langle 111 \rangle$ β directions.

gram analysis using ten ω precipitates, calculated with a bin size of 0.1 nm [10]. The large difference between the Mo contents of the β ($\sim 12\text{at}\%$) and the ω ($\sim 3\text{-}4\text{at}\%$) regions in this image indicates the substantial rejection of Mo from the growing ω precipitates during isothermal annealing at 475°C .

A filtered high-resolution HAADF-STEM image from the rapidly cooled Ti-9at%Mo sample, viewed long the $\langle 011 \rangle$ direction of the β matrix is shown in Fig. 2(a). This HAADF-STEM image exhibits regions of relatively brighter and darker contrast indicative of differences in atomic masses between these regions (Z-contrast). In some cases the darker regions of lower Z exhibit shifts in the atomic columns corresponding to the nanoscale embryos of the ω -like phase. Two such ω -like embryos are marked in both Fig. 2(a). In Fig. 2(b) an atom probe reconstruction is shown, depicting Ti-rich regions as an iso-concentration surface (Ti = 93 at%) together with the corresponding proximity histogram [10]. This proximity histogram shows Mo partitioning across this interface with $\sim 6\text{at}\%$ and $\sim 10\text{at}\%$ Mo in the solute-depleted and solute-rich regions respectively.

Fig. 3(a) is an enlarged HAADF-HRSTEM image showing the un-displaced and partially displaced atom columns representing the β matrix and an ω -like embryo respectively. The partially collapsed $\{111\}$ planes of the bcc (β) matrix are evident within the ω -like embryo in the supercell. In Fig. 3(b), we quantify the atomic displacements within the ω -like embryo with respect to the β matrix by plotting the column intensities along rows 1, 2, and, 3 as a function of distance along $\langle 111 \rangle$ β direction. For simplicity, the origin for each row has been transposed to overlap, and the structure transitions from β to ω -like as we move from left to right along the distance axis. The spacing between adjacent atomic columns along row-1 is $3d_{222}$, where d_{222} is the interplanar spacing between the $\{222\}$ planes of the β -structure. The collapse of the $\{111\}$ planes can be described as a displacement wave of wavelength $\lambda = 3d_{222}$ and a corresponding wave vector of $2/3 \langle 111 \rangle^*$ (reciprocal space) [11, 12]. Based on this formalism, complete

β to ω transformation corresponds to a longitudinal displacement wave of $0.5d_{222}$ amplitude. As seen in Fig. 3(b), the displacements of the atomic columns in rows 2 and 3 are in the range $0.16d_{222} - 0.2d_{222}$, progressively increasing on moving from left to right along the distance axis in Fig. 3(b) (from β to ω region). Consequently, the partial collapse of the $\{111\}$ planes, observed here, indicates a smaller amplitude of the displacement wave compared to that seen in full collapse. This is further illustrated by crystal motifs in Fig. 3(b) depicting B and C planes forming a partially collapsed ω -like structure.

Density Functional Theory Calculations: Systems with 0at.%, 8.33at.%, and 16.66at.% Mo in Ti were studied. Molybdenum atoms were added on collapsing $\{111\}$ planes of β and ω titanium and these structures relaxed using Vienna Ab-initio Simulation Package (VASP) [13–15] and projector augmented wave (PAW) pseudopotentials [16]. The generalized gradient approximation of Perdew, Burke, and Ernzerhof was used [17]. A plane-wave kinetic-energy cutoff of 400 eV and $3 \times 3 \times 5$ k-point mesh size was used to ensure an accuracy of to 1 meV/atom. For titanium we treat the 3p states as valence states in addition to the usual 4s and 3d states to increase accuracy. Nudged elastic band (NEB) calculations[18] with constant cell volume yield the minimum energy pathway (MEP) for the β to ω transformation shown in Fig. 4(a). The dependence of results on system size was examined by studying systems with 12, 24, and 48 atoms in the super cell, and energy barriers are accurate to about 2 meV/atom. While there is no activation barrier for β to ω transformation in the pure Ti system, we see a local energy minimum for Ti-8.3at.% Mo system along the MEP corresponding to an average partial collapse of $\{222\}$ planes. The normalized interplanar spacing for this local minimum structure is 0.25 from NEB, in agreement with experimental value of 0.20. Interestingly, $\langle 111 \rangle$ atom columns with Mo atom do not collapse while a neighboring parallel $\langle 111 \rangle$ column with Ti does so. For full collapse to occur, Mo atoms must diffuse out of the omega region. Such a partially collapsed structure is energetically favored over a fully

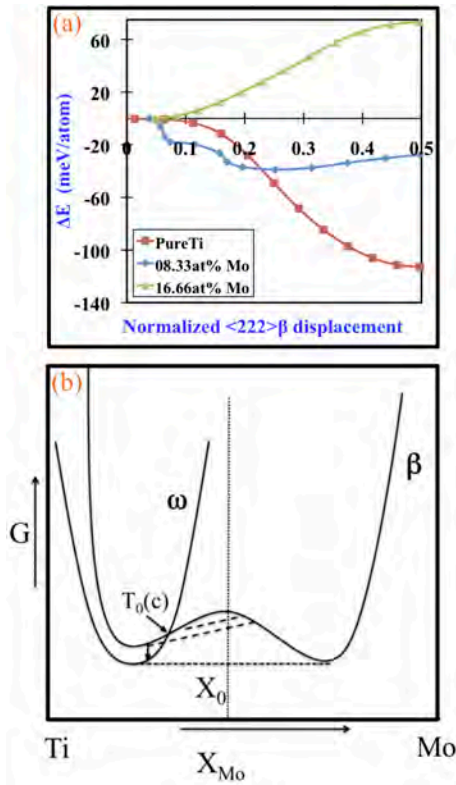


FIG. 4: (a) Nudged elastic band (NEB) results plotted for 24 atom supercell systems with 0at.%, 8.33at.%, and 16.66at.% Mo in Ti. ΔE is relative energy of the system along the minimum energy path with β phase taken as reference. (b) A schematic plot of Gibbs free energy versus composition for Ti-Mo binary system.

collapsed structure when we have Mo atoms in the cell.

We propose the following mechanism for the formation of embryonic ω within the β matrix. An undercooled alloy of composition Ti-9at.%Mo presumably has a free energy lying within the miscibility gap (also within the spinodal) of the β phase as shown for the composition marked X_0 in Fig4(b), and consequently is unstable with respect to compositional fluctuations. Subsequent diffusional rejection of Mo from the growing embryos leads to an increase in the degree of collapse of $\{111\}$ bcc planes eventually forming a fully developed hexagonal ω structure. As compositional fluctuations grow in amplitude and wavelength, the solute (Mo) depleted regions within the β phase cross the $T_0(c)$ point of intersection of the β and ω free energy curves. These solute-depleted regions now become metastable (or unstable) with respect to the structural instability causing partial collapse of the $\{111\}$ β planes and the formation of ω -like embryos. This leads to nanoscale, compositional clustering (phase separation) into Mo-enriched and Mo-depleted regions, presumably by a second order spinodal process as indicated by the dotted lines in Fig4(b). Systematic correlation between the local atomic displacements and the composition of the solute-depleted regions in Ti-Mo alloys is currently

being carried out using DFT calculations.

Summary: By coupling aberration-corrected HAADF-STEM with atom probe tomography and DFT calculations, the early stages of phase separation (compositional clustering) and consequent displacive collapse of $\{111\}$ bcc planes within the solute-depleted regions of the β matrix of Ti-Mo alloys have been established. These results provide novel insights into the mechanisms of solid-state transformations in metallic systems by capturing the earliest stages of nucleation at atomic to near atomic spatial and compositional resolution. A new class of mixed mode diffusional-displacive phase transformations involving a composition-dependent displacive component emerges from this mechanism.

The National Science Foundation (award# 6701956, 0700828, and 0846444) and US Air Force Research Laboratory funded this work. Experimental facilities at UNT's Center for Advanced Research and Technology and OSU's Center for the Accelerated Maturation of Materials, and the Talon Linux cluster at UNT were used.

- [1] S. Banerjee & P. Mukhopadhyay, *Phase Transformations – Examples from Ti and Zr Alloys* (Pergamon, Oxford, 2007).
- [2] P. D. Frost, W. M. Parris, L. L. Hirsch, J. R. Doig, & C. M. Schwartz, Trans. Amer. Soc. Metals **46**, 231243 (1954).
- [3] R. R. Boyer, G. Welsch, & E. W. Collings, *Materials Properties Handbook: Ti Alloys* (ASM Handbook, 1994).
- [4] I. Bakonyi, H. Ebert, & A. I. Liechtenstein, Phys. Rev. B **48**, 7841 (1993).
- [5] G. B. Grad, P. Blaha, J. Luitz, & K. Schwarz, Phys. Rev. B **62**, 1274312753 (2000).
- [6] D. D. Fontaine, N. E. Paton, & J. C. Williams, Acta Metall. **19**, 1153 (1971).
- [7] J. C. Williams, D. D. Fontaine, & N. E. Paton, Metall. and Mater. Trans. B **4**, 27012708 (1973).
- [8] M. K. Miller, K. F. Russell, K. Thompson, R. Alvis, & D. J. Larson, Micro. and Micro. **13**, 428 (2007).
- [9] A. Devaraj, R. E. A. Williams, S. Nag, R. Srinivasan, H. L. Fraser, & R. Banerjee, Scripta Mater. **61**, 701 (2009).
- [10] O. C. Hellman, J. A. Vandenbroucke, J. Rusing, D. Isheim, & D. N. Seidman, Micro. and Micro. **6**, 437 (2000).
- [11] D. D. Fontaine, Acta Metall. **18**, 275 (1970).
- [12] D. D. Fontaine & O. Buck, Philos. Mag. **27**, 967983 (1973).
- [13] G. Kresse & J. Hafner, Phys. Rev. B **47**, 558 (1993).
- [14] G. Kresse & J. Hafner, Phys. Rev. B **49**, 14251 (1994).
- [15] G. Kresse & D. Joubert, Phys. Rev. B **59**, 1758 (1999).
- [16] P. E. Blchl, Phys. Rev. B **50**, 17953 (1994).
- [17] J. P. Perdew, K. Burke, & M. Ernzerhof, Phys. Rev. Lett. **78**, 1396 (1997).
- [18] H. Jönsson, G. Mills, & K. Jacobsen, *Classical and Quantum Dynamics in Condensed Phase Simulations* (World Scientific, Singapore, 1998), 1st edition.